Specialized Algorithms for Spectrum Surveys

Heather Ottke [1], Chriss Hammerschmidt [2]

Institute for Telecommunications Sciences (NTIA/ITS)

325 Broadway St.- Boulder, CO 80305

[1] hottke@its.bldrdoc.gov

[2] chammerschmidt@its.bldrdoc.gov

Abstract—**With increased demand in the radio spectrum, there have been multiple recent campaigns to quantify spectrum occupancy through measurements. These measurements can pose many challenges, one of which is created by impulsive noise. Below 500 MHz, impulse noise can be particularly prominent and mimic narrowband LMR emissions during measurements that use common swept spectrum measurement techniques.**

This paper discusses methods to properly measure the intentionally radiated signals in the environment while minimizing measurement of unintentional emissions and describes processing algorithms that may be used to assist in distinguishing between LMR emissions and impulsive noise.

I. Introduction

Rapid growth in wireless applications in the last twenty years has placed an increased demand on the radio frequency (RF) spectrum. The spectrum is a limited resource that allows a tremendous number of people to perform a wide variety of complex functions ranging from broadcasting music and television to being able to view inside the human body to detect tumors, diagnose diseases such as cancer, and discover abnormalities [1].

Various types of signals are transmitted to accomplish these functions. Some of these signals are transmitted by land-mobile radios (LMRs), radars, satellites, fixed point-to-point microwave links, cellphones and broadcasters, as well as by Industrial Scientific and Medical (ISM) devices. Performing spectrum surveys is critical to understanding the true nature of the signals that surround us in our everyday lives by indicating how and when they are utilized. The Institute for Telecommunication Sciences (ITS) has measured the RF spectrum for usage statistics [2]–[4], radar characteristics [5], and general occupancy measurements [6]–[9]. Most of these measurements use specialized algorithms to characterize various aspects of the signals in each band so that an accurate representation of the spectrum can be identified.

II. Measurement challenges

Many methods can be used to measure the various aspects and characteristics of the spectrum. The most effective approach is to have knowledge of the transmitter characteristics so that the most appropriate measurement equipment and parameters can be chosen. If the measurement method is not considered carefully, artifacts may be mistaken for real signals in the measured spectrum. Each transmitter presents a unique challenge, and special measurement considerations must be made on a band-by-band basis.

For example, the characteristics that must be considered for radar emissions are the short pulse periods, the low duty cycles, the narrow beam-widths of transmitting antennas and the radar's rotation through space. If measured with a frequency-swept algorithm, there is no assurance that the main beam of the radar antenna will be pointed at the measurement system at the time the data is acquired; therefore, it is possible that most of the measured data will come from the side-lobes and back-lobes of the antenna, which will show a reduced power radar spectrum. Radars require specialized measurement algorithms to assure the maximum pulse power is measured at each frequency step throughout the radar band.

Other measurements present different challenges. Satellite measurements may need to be tailored to orbital information and low received signal. If an algorithm is not created to reposition a high-gain antenna to scan the signal space as the satellite passes overhead, the signal could be completely missed.

Point-to-point microwave links are engineered for line-of-sight operation with narrow-beam antennas. Measurements of point-to-point microwave links may present challenges if the measurement system is not in direct line with the transmit path. If not aligned within the narrow beam-width of the antenna, the receiver could miss the signal completely. Foliage may also pose a problem since at most of the microwave frequencies obstructions can significantly attenuate the signal power.

All of these challenges can be overcome with specialized measurement and processing algorithms to extract a more accurate representation of the intentionally radiated signal environment in each band.

III. Case study: Specialized measurements of LMR signals

This paper will focus on measurement and processing techniques associated with measuring emissions from LMR transmitters. Land mobile radios are used by public safety, large vehicle fleets, manufacturers, utilities, railroads and a wide variety of other businesses [10]. The transmitters include base stations and portable devices, including handhelds and mobiles. The mobiles are mounted in vehicles or aircraft. The typical LMR transmission time is at least one second and usually no more than three minutes [11]. LMR transmissions are channelized in multiple spectrum bands with bandwidths of 6.25 kHz, 12.5 kHz, 15 kHz, 20 kHz, 25 kHz or 30 kHz. LMRs have very low duty-cycles and the power levels of LMRs may vary due to their mobile operation. Some LMRs

978-1-4673-2060-3/12/$31.00 ©2012 IEEE

operate in spectrum allocations below 500 MHz where impulsive noise can be significant.

Impulsive noise originates from natural electrical discharges within the atmosphere associated with thunder storms (atmospheric noise), as well as from man-made sources including power line corona discharge, electric machinery, automobile ignition, construction equipment, digital networks, switching power supplies, alarms and horns, and many other sources [12]–[14]. Impulsive noise can be characterized by its short duration, high intensity and abrupt onset and decay [12]. It can mask existing signals by raising the noise floor above the signal level.

Due to the intermittent behavior, short time duration and variable power levels of both impulsive noise and LMR signals, impulsive noise may be mistaken for an LMR emission. To differentiate between the two we can take into account the shorter duration as well as the frequency-domain characteristics of an impulse function. In theory, the Dirac delta is infinitely wide in the frequency-domain. Applying this theory indicates the impulsive noise will be a wideband signal in the frequency-domain causing the noise floor of the entire band to be raised. An LMR signal on the other hand is narrowband in the frequency-domain; LMR signals would not raise the noise floor in the entire band unless every channel was occupied by LMRs with constant transmissions.

Specialized measurement algorithms are required to differentiate this impulsive noise from actual intentionally radiated signals.

A. Measurement Configuration & Considerations

Measurements at ITS are performed using the fourth generation Radio Spectrum Measurement System (RSMS-4G) truck shown in Fig. 1. The truck is equipped with 60 dB of RF shielding, racks to mount equipment, and masts to mount and elevate antennas. Our most recent survey was conducted in Arvada, Colorado, on a site overlooking the surroundings with an approximate elevation of 1700 meters (5600 feet).

Fig. 1. Radio Science Measurement System (RSMS) 4G Truck

Specialized configurations are used depending on the types of emissions transmitted in a particular band. Fig. 2 displays a configuration that we use to measure LMR signals below 500 MHz. As shown, our system consists of a discone antenna which provides 0 dBi gain over 25 MHz to 1300 MHz, two preselectors (one mounted on the mast and another located inside the truck), a spectrum analyzer, and a computer.

Both preselectors contain a noise diode for system calibrations and a variable attenuator to adjust the dynamic range, as well as filters and amplifiers for analog signal processing. The mast-mounted preselector is used only for calibration purposes in this configuration. All preselection is accomplished in the lower preselector inside the truck. The parameters of the spectrum analyzer are set by computer software which also saves the acquired data to the hard drive.

Attenuation values were selected that would reduce the noise figure of the system while optimizing the dynamic range. The system is designed so that the spectrum analyzer would compress before the low-noise amplifier (LNA) located inside the preselector. The spectrum analyzer has built-in functions that readily detect overloads and report them to the computer.

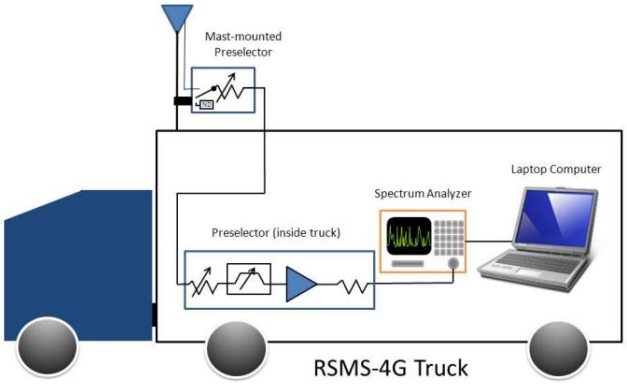

Fig. 2. System Configuration for LMR measurement

B. Calibration Method

Calibrations are performed before, at intervals during, and after a measurement to ensure that the system is operating as intended with the expected gain and noise figure. A noise diode is switched into the system in place of the antenna and a Y-factor calibration method is performed [15]. The received noise power of the system is measured as a function of frequency. The gain and noise figure are calculated from the measured power. For LMRs transmitting under 500 MHz, the system is typically designed to have approximately 35 dB gain with a 7 dB noise figure.

C. Measurement Algorithm for LMRs

As mentioned previously, the intermittent use and low duty cycle behavior of LMR emissions can be mimicked by impulsive noise when measured using a swept mode of a spectrum analyzer. Using the fast Fourier transform (FFT) method described in the next paragraph reduces or eliminates impulsive noise from the measurement while preserving the traces of intentional transmissions

The FFT method involves acquiring the spectrum in the time-domain, digitizing the time sample and using FFT processing to convert the complex baseband in-phase (I) and quadrature-phase (Q) data into the frequency-domain.

The current LMR measurement algorithm consists of acquiring five rapid traces in 0.9 s and performing real-time median-of-five processing. This is accomplished by applying median processing of power levels for each frequency shortly after acquiring five power traces at a specific band. If impulsive noise is present in fewer than three out of the five traces, the impulses are eliminated since the median picks the middle power level of five values.

All five traces must be acquired in approximately one second, since LMR transmissions generally last one second or longer, while the measured impulsive noise occurs over a much shorter period of time (as short as 160 μs in a 6.25 kHz resolution bandwidth (RBW)). A signal lasting less than one second does not represent a reasonable voice transmission since very little can be said in less than one second. To acquire the five traces in more than one second may result in the exclusion of short LMR transmissions. If the five traces are acquired too rapidly, a single impulse may be represented by more than three traces, and prevent its exclusion through processing.

Each band is 4–6 MHz wide and measured for 1.1 minutes until moving to the next band.

D. Post-Processing Algorithms

Batch processing is performed to create the three plots in Figs. 3–6. The top plot displays the maximum, mean, median, and minimum power levels. The middle plot is a time-energy contour plot and the bottom plot displays the percentage of time a certain power level is exceeded. All plots will be discussed in greater detail in the following paragraphs.

The data from all of the traces acquired during the measurement are processed to create histograms of the number of occurrences of power levels at each frequency. Each bin is divided by the total number of traces to give probabilities and then incrementally summed to produce a cumulative distribution. From this, a complementary cumulative distribution function (CCDF) is produced, after which the statistics shown in the top and bottom graph are determined.

Power levels on the y-axis of the top and bottom graphs are referenced to the antenna input and displayed as field strength in units of dB μV/m.

The top plot displays the maximum, mean, median, and minimum (M4) field strength statistics for all power-level values measured at each frequency throughout the spectrum survey. Except for the mean, the statistics are determined from the CCDF by finding the highest value measured, the smallest value measured, and the value above which 50% of the power levels occur. The mean system noise is calculated using calibration information and plotted along with the M4 statistics to help determine whether noise observed between obvious signals is due to system noise or other sources such as environmental noise.

The middle graph is a contour plot. The vertical axis displays time and the contours show 20 levels of color indicating power levels; blue indicates a lower power level and red a strong power level. A threshold is created referenced to the mean system power level and only data above this threshold are displayed on the graph. For LMR bands under 500 MHz, the threshold value is typically set to the level at which the power on the y-axis is exceeded 0.1% of the time. When high signal levels exist in the band, this is adjusted so that important signal characteristics are shown in the time-frequency plot. Each data point on the time versus frequency graph is the maximum trace value in each measurement interval (i.e. 1.1 minutes for LMR).

There are advantages to using thresholds. Thresholds clearly identify the important time-varying characteristics; while concealing low-level signals. Not using a threshold allows noise to overwhelm the middle plot, obscuring time-varying activity. For Fig. 5, the threshold is 8 dB above the mean system noise since there is a probability of less than 0.1% that system noise will exceed 8 dB above the mean system noise for this particular measurement.

The bottom plot is a percent probability graph that provides additional information that the other two plots are not able to extract. This plot can assist in differentiating signal types and shows the percentage of time that a signal exceeds the field strength given on the y-axis. It also displays low-level signals that reside in the noise. It is possible to observe the low-level signals due to the statistical characteristics of Gaussian noise compared to the statistics of other signal types. The percentage of time that a certain power level is exceeded is displayed on the vertical axis. This plot assists in identifying a frequency that may be occupied, but in which signals are actually present for only a short fraction of the time. Probability values of 0.0003%, 0.0355%, 0.6658%, 4.233%, 13.60%, 28.60%, 45.19%, 60.58%, 72.89%, 81.91%, 88.17%, 92.35% were chosen since these values are evenly spaced on a Rayleigh scale. Gaussian noise shows power levels evenly distributed corresponding to these power values. For instance, in the bottom graph of Fig. 6, in between obvious signals the system noise is represented by evenly spaced lines. Any disturbance in this evenly distributed pattern is indicative of non-Gaussian behavior, such as some type of signal or impulsive noise. This method of presenting the measurement results allows the detection of weak signals very close to the noise floor.

In the event that impulsive noise is present in more than three out of the five traces, a second method is used to eliminate the remaining impulses. A threshold factor is used to determine if a certain percentage of data points representing noise are elevated 3 dB above the threshold. Various threshold factors are applied to each individual trace based on the percentage of intentionally radiated emissions that exist in the band. For instance, a 50% threshold factor would be used to determine if 50% of the noise is within 3 dB of the threshold, indicating the presence of impulsive noise. If this statement is true then the entire trace is thrown out.

Fig. 3. 50% Threshold Factor

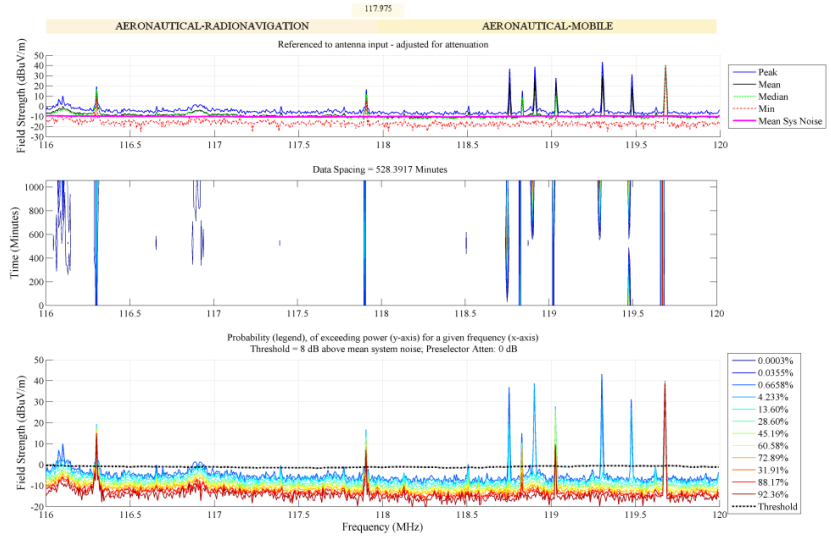

Fig. 4. 5% Threshold Factor

Fig. 3 shows the effect of a 50% threshold factor. Notice in the middle plot how the noise is dominant across the frequency band obscuring the intentionally radiated activity. In contrast, Fig. 4 shows that if the threshold factor is changed to 5%, this minimizes the effects of impulsive noise and allows the observation of the intentionally radiated signal space. In this case, approximately 5% of the band was occupied by intentional signals.

E. Measurement Comparisons

While measuring the LMR spectrum below 500 MHz, a comparison was performed between the FFT method using a median-of-five processing (described in Section C) and a swept spectrum measurement consisting of simply sweeping through the spectrum without the median-of-five processing. The latter was measured with the same RBW and swept multiple times for approximately the same length of time as the FFT method.

By acquiring data in the time-domain, the time record can hopefully capture the entire spectral content of a signal in that specific slice of time. Swept analyzers, on the other hand, generally have a slower acquisition rate, so portions of fast-changing signals could be missed [16].

Fig. 5 shows the results from the swept spectrum measurement without median-of-five processing. Looking at the mean measured power and the mean system noise between obvious RF signals in the top graph, one can see that the curve for the mean system noise is significantly below the curve for the mean RF power. This is indicative of noise originating from something other than the system noise. In addition, one can see in the bottom graph that there is an uneven distribution in spacing of the curves in between signals. This is indicative of impulsive noise, since Gaussian system noise

is evenly spaced with a narrower spread. Impulsive noise typically results in a wider spread of the upper curves associated with lower probability values.

Fig. 6 displays the results of the FFT measurement method using median-of-five processing. The mean system noise plot on the top graph lies relatively close to the plot for the measured RF powers. In addition, the noise measured between obvious signals shows evenly distributed probability lines in the lower graph. Both of these observations are indicative of Gaussian noise, as opposed to environmental RF noise.

Comparing Fig. 5 with Fig. 6, it is evident that the median-of-five processing method produces a better representation of the true nature of the radio environment. In Fig. 5, the data gives the false impression that the spectrum in this band is used at least part time throughout the entire band. The time-varying plot is almost completely obscured by the effects of impulsive noise. In Fig. 6, we get a much clearer and more realistic view of actual usage of the band. Also notice, in Fig. 6, that some of the very weak signals that are close to the system noise floor are obscured by the impulsive noise when displayed in Fig. 5.

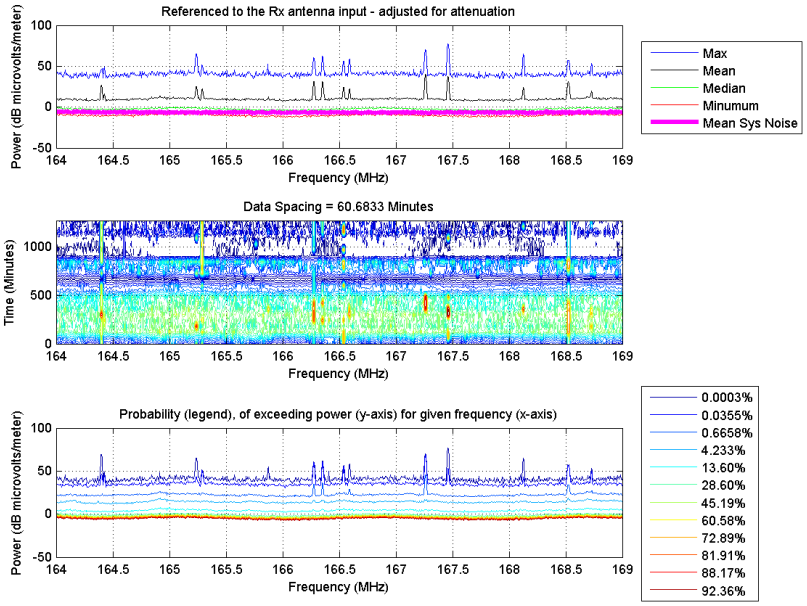

Fig. 5. Swept LMR Measurement – includes impulsive noise

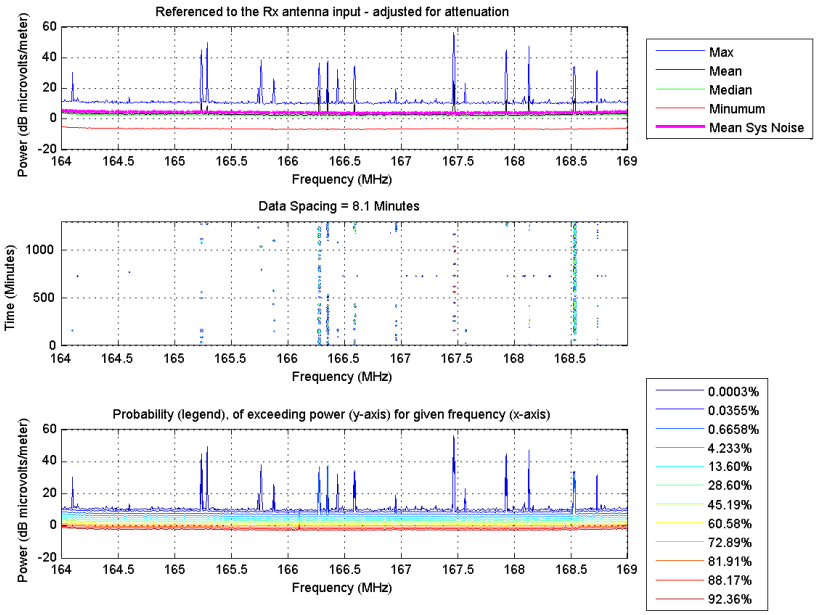

Fig. 6. Basic Mode LMR Measurement – impulsive noise removed

IV. Conclusion

The wide varieties of applications that occupy the RF spectrum have transmitters which dramatically differ in the way that they operate. With the increase in technologies being implemented, it is essential to investigate the transmitters expected to be in a frequency band so that important transmitter characteristics can be determined, including modulation schemes, duty cycle, spatial features corresponding to angular rotation of a transmitter, beam-width, and transmit power. Once the transmitter parameters are noted, measurement decisions can be made depending on the information the measurement is intended to obtain. Important considerations such as measurement equipment limitations and environmental factors must not be ignored. Specialized measurement and processing algorithms must be created to obtain the most accurate representation of the intentionally radiated signal environment.

An accurate determination of the RF spectrum is essential, otherwise, incorrect policy decisions could be made based on measurements that attempt to quantify the RF spectrum, yet might not do so accurately.

Acknowledgment

We would like to thank Bob Johnk for his encouragement in writing and presenting this paper, Randy J. Hoffman for his technical contributions and continued support and Lilli Segre for her editorial expertise.

References

[1] RadiologyInfo.org, "What are the benefits of CT scans?" Aug 2011. <http://www.radiologyinfo.org>, accessed on Feb. 26, 2012.

[2] R.J. Matheson, "Spectrum usage for the fixed services," NTIA Report 00-378, Mar. 2000.

[3] J.A. Wepman, R.J. Matheson, K.C. Allen and R.J. Achatz, "Spectrum usage measurements in potential PCS frequency bands," NTIA Report 91-279, Sep. 1991.

[4] F.H. Sanders, G.R. Hand, and V.S. Lawrence, "Land mobile radio channel usage measurements at the 1996 Olympic Games," NTIA Report 98-357, Feb 1998.

[5] F.H. Sanders, R.L. Hinkle and B.J. Ramsey, "Measurement procedures for radar spectrum engineering criteria (RSEC)," NTIA Report 05-420, March 2005.

[6] J.R. Hoffman, R.J. Matheson, and R.A. Dalke, "Measurements to characterize land mobile channel occupancy for Federal bands 162–174 MHz and 406–420 MHz in the Washington, D.C., area," NTIA Report 07-448, Jul. 2007.

[7] F.H. Sanders and V.S. Lawrence, "Broadband spectrum survey at Denver, Colorado," NTIA Report 95-321, Sep. 1995.

[8] F. H. Sanders, B.J. Ramsey, and V.S. Lawrence, "Broadband spectrum survey at San Francisco, California, May–June 1995," NTIA Report 99-367, Jul. 1999.

[9] F. H. Sanders, B.J. Ramsey, and V.S. Lawrence, "Broadband spectrum survey at San Diego, California," NTIA Report 97-334, Dec. 1996.

[10] M. Farquhar, D. Wye, J. Borkowski, E. Johnson and S. Fleming, "Private Land Mobile Radio Services: Background," Federal Communications Commission, 1996. <http://www.wireless.fcc.gov/reports/documents/whtepapr.pdf>, accessed on April 1, 2012.

[11] P. Lunness, Land Mobile Radio Systems, Radio System Design, Daniels Electronics, Ltd., TG-002, Revision 2-0-0, Oct. 2009. <http://www.danelec.comhttp://www.danelec.com/TG-002-2-0-0%20Radio%20System%20Design.pdf>, accessed on Mar. 28, 2012.

[12] R.A. Niedzielski, "Environmental Impulse Noise Study," Minnesota Pollution Control Agency Final Report, May 1991. <http://www.nonoise.org/library/impulse/impulse.htm>, accessed on Apr. 25, 2012.

[13] R.J. Achatz and R.A. Dalke, Man-made noise power measurements at VHF and UHF frequencies," NTIA Report 02-390, December 2001.

[14] R.A. Dalke, "Radio Noise," in *Wiley Encyclopedia of Electrical and Electronics Engineering*, J. Webster, Ed., New York: Wiley, 2005, pp. 128–140.

[15] Agilent Technologies, "Noise Figure Measurement Accuracy – The Y-Factor Method," *Application Note 57-2*, May 2010.

[16] R. Witte, *Spectrum and Network Measurements*, Saddle River, NJ: Prentice-Hall, Inc., 1993, pp. 62–105.